more sensitive to DNA damage than their parental AGM fibroblasts.

We carried out inverse PCR analyses to identify the integration sites of the lentiviral vectors expressing reprogramming factors in CM DGs. OCT 3/4-, SOX2-, KLF4-, and c-MYC-expressing lentiviral vectors were integrated into 5, 12, 5, and 9 genomic sites, respectively (Fig. S6b, Table S1). The possibility that multiple integrations of lentiviral vectors into the genome caused chromosome instability, leading to the formation of CM DGs, could therefore not be excluded.

Dependence of CM DGs growth on c-MYC and bFGF signalings. To address the question of whether proliferation of CM DGs was dependent on reprogramming factors, we observed the proliferation rate after suppression of each reprogramming factor by shRNA (Fig. S10). Suppression of c-MYC or all four reprogramming factors greatly inhibited the proliferation of CM DGs, indicating that the growth of CM DGs was highly dependent on c-MYC (Fig. 5a).

The proliferation of human ESCs is known to be promoted by bFGF signaling.[23] We examined the possibility that the growth of CM DGs might also be enhanced by bFGF signaling by analyzing the proliferation of CM DGs cultured in medium with or without bFGF. The growth of CM DGs was highly dependent on bFGF (Fig. 5b). Consistent with these results, BGJ398, an inhibitor for FGFR 1 to 4, remarkably inhibited the growth of CM DGs in a dose-dependent manner (Fig. 5c). Moreover, FACS analyses revealed that the sub-G_1 population, representing dead cells, was increased in the presence of BGJ398 (Fig. S11). It should be emphasized that the IC_{50} of BGJ398 (59 nM) was lower for CM DGs than for their parental AGM fibroblasts and control CM skin fibroblasts (Fig. 5d), indicating higher sensitivity of CM DGs. These results suggested that the growth of CM DGs was dependent on bFGF signaling, and therefore FGFR inhibitor could be used to control the growth of the reprogramming factor-induced tumor.

Discussion

In this study we investigated the characteristics of ARCs and CM DGs generated in the reprogramming process of CM AGM fibroblasts by Yamanaka factors.

A normal iPSC line of iPS A cells, showed the expression of ES markers, pluripotency, and flattened morphology, like human iPSCs.[20] In contrast, ARCs showed sphere-like structures, like mouse iPSCs.[1] This morphological difference between iPS A cells and ARCs might be useful to select "true" iPSCs derived from CM, although the underlying molecular mechanisms responsible for this morphological difference remain unknown.

We found, by microarray analyses, that the gene expression pattern in ARCs was more similar to that in iPS A cells than that in AGM fibroblasts, suggesting that reprogramming processes have been done in ARCs by the transduction of reprogramming factors. We also found that genes such as *ZFHX4*, *NFIX*, *HOXC8*, *STMN2*, and *CXORF67* were highly expressed in ARCs. It should be noted that, among these, *HOXC8* is known to be a transcriptional factor related to tumorigenesis.[24] Therefore, these candidates of markers might be useful to predict the tumorigenic potential of iPSCs. Further evaluation is required to confirm our hypothesis.

The original AGM fibroblasts had an abnormal marker chromosome (mar; Fig. 2a, left panel). Although tumor formation was not evident caused in SCID mice (data not shown), this chromosome instability might also be one of the inducers of

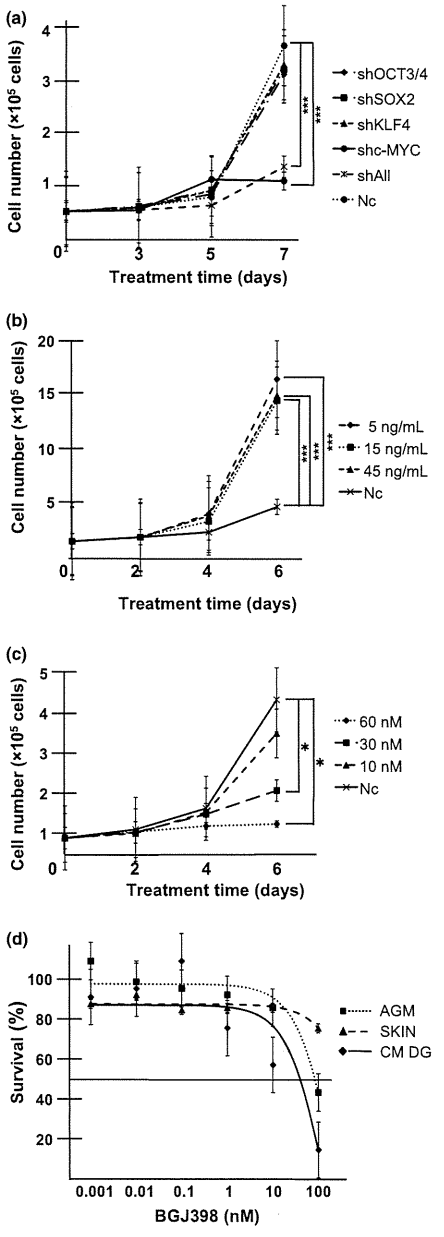

Fig. 5. Dependence of common marmoset dysgerminoma-like (CM DG) cell growth on c-MYC and basic fibroblast growth factor (bFGF) signaling. (a) Inhibition of CM DG growth by knockdown of c-MYC. Cells (3×10^4) were seeded on 24-well plates and transduced with shRNA targeting OCT3/4, SOX2, KLF4, c-MYC, or all reprogramming factors (shAll). Cell growth curves were analyzed by cell counts at the indicated time points. Results are shown as means ± SD. ***$P < 0.001$. Nc, negative control (mock vector). (b) Growth rate of CM DGs was promoted by the addition of bFGF. Cells were cultured in the presence or absence (Nc) of bFGF. Cell numbers were counted at the indicated time points. Results are shown as means ± SD. ***$P < 0.001$. (c) FGFR inhibitor suppressed CM DG growth. Cells were cultured in the presence or absence (Nc) of the FGFR1-4 inhibitor BGJ398; bFGF was added at 5 ng/mL. Cell numbers were counted at the indicated time points. Results are shown as means ± SD. *$P < 0.05$. (d) CM DGs, aorta-gonado-mesonephros fibroblasts (AGM), and CM skin fibroblasts (SKIN) were treated with different concentrations of BGJ398 for 3 days, and the growth-inhibitory effects were analyzed by MTS assay. The IC_{50} for CM DGs was lower than those for parental AGM fibroblasts and control CM skin fibroblasts. Results are shown as means ± SD.

carcinogenesis during the reprogramming process. Thus, needless to say, to generate "safe" iPSCs, validation of the karyotype of the original cells is needed. Moreover, ARCs lost chromosome 4q and X or Y, and possessed an abnormal marker chromosome (mar). Various tumor suppressors including human tumor suppressor gene 1, large tumor suppressor 1 and P36 transformed follicular lymphoma gene have been identified on chromosome 4q in CM cells (Table S2), suggesting that loss of these tumor suppressors might have induced the transformation of CM AGM fibroblasts during reprogramming, although the possibility that translocation of chromosome 4q occurred during the reprogramming process caused the transformation of cells could not be excluded.

It is also possible that the continuous activation of ectopically-transduced transcription factors, including the oncogene *c-MYC*, might have contributed to cell transformation, as described previously.[25,26] Indeed, CM DGs overexpressed c-MYC, and their growth was highly dependent on c-MYC expression, suggesting that downregulation of c-MYC might represent a possible strategy for inhibiting the growth of reprogramming factor-related tumors.

Insertional mutation caused by the integration of lentiviral vectors into the genome might also have promoted cell transformation. Lentiviral vectors expressing reprogramming factors were integrated into at least 31 different genomic sites in CM DGs, some of which were in the vicinity of protein-encoding genes. Moreover, the expression of reprogramming factors transduced by lentiviral vectors continued for over a year in ARCs (data not shown). A safer method, without genome integration, is therefore required for the delivery of reprogramming factors to somatic cells to generate iPSCs applicable for transplantation therapies. Although Sendai virus vectors or transfection of DNA or mRNA may be safer methods,[27] these are lengthy processes that can take more than 1 month to obtain iPSCs,[28] which could also cause stress and lead to genomic instability and subsequent tumor formation. More sophisticated, safer, and more rapid methods of reprogramming might be desirable.

Common marmoset DGs resembled human dysgerminomas in terms of both their pathology and sensitivity to irradiation and DNA-damaging agents.[21,22] In addition, the growth of CM DGs was significantly inhibited by an FGFR1-4 inhibitor. Therefore irradiation, chemotherapy, and FGFR1-4 inhibitors might be effective strategies for controlling human dysgerminomas, and also for tumors that develop in patients treated with iPSC-based therapies.

Acknowledgments

We thank Hiroyuki Miyoshi (Riken, Tsukuba, Japan) for providing lentiviral vectors, Norihiko Kinoshita (Kyushu University, Fukuoka, Japan) and the Laboratory for Technical Support (Medical Institute of Bioregulation, Kyushu University) for their technical assistance, Michiko Ushijima for administrative assistance, and members of Prof. Kenzaburo Tani's laboratory for constructive criticisms. This work was supported by grants from the Project for Realization of Regenerative Medicine (K.T., 08008010) and Kakenhi (T.M., 23590465) from the Ministry of Education, Culture, Sports, Science and Technology, Japan.

Disclosure Statement

The authors have no conflicts of interest.

Abbreviations

AGM	aorta-gonado-mesonephros
AP	alkaline phosphatase
ARC	abnormally reprogrammed cell
bFGF	basic fibroblast growth factor
CM	common marmoset
DG	human dysgerminoma-like cell
ESC	embryonic stem cell
FGFR	fibroblast growth factor receptor
iPSC	induced pluripotent stem cell
K	KLF4
M	c-MYC
MMC	mitomycin C
O	OCT3/4
S	SOX2

References

1 Takahashi K, Yamanaka S. Induction of pluripotent stem cells from mouse embryonic and adult fibroblast cultures by defined factors. *Cell* 2006; **126**: 663–76.
2 Okita K, Yamanaka S. Induced pluripotent stem cells: opportunities and challenges. *Philos Trans R Soc Lond B Biol Sci* 2011; **366**: 2198–207.
3 Okita K, Ichisaka T, Yamanaka S. Generation of germline-competent induced pluripotent stem cells. *Nature* 2007; **448**: 313–U1.
4 Ohm JE, Mali P, Van Neste L *et al.* Cancer-related epigenome changes associated with reprogramming to induced pluripotent stem cells. *Cancer Res* 2010; **70**: 7662–73.
5 Wernig M, Meissner A, Cassady JP, Jaenisch R. c-Myc is dispensable for direct reprogramming of mouse fibroblasts. *Cell Stem Cell* 2008; **2**: 10–2.
6 Okita K, Nakagawa M, Hong HJ, Ichisaka T, Yamanaka S. Generation of mouse induced pluripotent stem cells without viral vectors. *Science* 2008; **322**: 949–53.
7 Judson RL, Babiarz JE, Venere M, Blelloch R. Embryonic stem cell-specific microRNAs promote induced pluripotency. *Nat Biotechnol* 2009; **27**: 459–61.
8 Lin TX, Ambasudhan R, Yuan X *et al.* A chemical platform for improved induction of human iPSCs. *Nat Methods* 2009; **6**: 805–U24.
9 Madonna R. Human-induced pluripotent stem cells. in quest of clinical applications. *Mol Biotechnol* 2012; **52**: 193–203.
10 Lunn SF. Systems for collection of urine in the captive common marmoset, *Callithrix-Jacchus*. *Lab Anim* 1989; **23**: 353–6.
11 Marumoto T, Tashiro A, Friedmann-Morvinski D *et al.* Development of a novel mouse glioma model using lentiviral vectors. *Nat Med* 2009; **15**: 110–6.
12 Tomioka I, Maeda T, Shimada H *et al.* Generating induced pluripotent stem cells from common marmoset (*Callithrix jacchus*) fetal liver cells using defined factors, including Lin28. *Genes Cells* 2010; **15**: 959–69.
13 Foster KW, Frost AR, McKie-Bell P *et al.* Increase of GKLF messenger RNA and protein expression during progression of breast cancer. *Cancer Res* 2000; **60**: 6488–95.
14 Gustafson WC, Weiss WA. Myc proteins as therapeutic targets. *Oncogene* 2010; **29**: 1249–59.
15 Vogelstein B. Genetic instabilities in human cancers. *Biophys J* 1999; **76**: A135–A.
16 Sasaki E, Hanazawa K, Kurita R *et al.* Establishment of novel embryonic stem cell lines derived from the common marmoset (*Callithrix jacchus*). *Stem Cells* 2005; **23**: 1304–13.
17 Li XJ, Du ZW, Zarnowska ED *et al.* Specification of motoneurons from human embryonic stem cells. *Nat Biotechnol* 2005; **23**: 215–21.
18 Liao JY, Marumoto T, Yamaguchi S *et al.* Inhibition of PTEN tumor suppressor promotes the generation of induced pluripotent stem cells. *Mol Ther* 2013; **21**: 1242–50.
19 Tumor of the ovary, Maldeveloped Gonads, Fallopian tube, and Broad Ligament., 1998; 239–65.
20 Ulbright TM. Germ cell tumors of the gonads: a selective review emphasizing problems in differential diagnosis, newly appreciated, and controversial issues. *Mod Pathol* 2005; **18** (Suppl 2): S61–79.

21 Brewer M, Gershenson DM, Herzog CE, Mitchell MF, Silva EG, Wharton JT. Outcome and reproductive function after chemotherapy for ovarian dysgerminoma. *J Clin Oncol* 1999; **17**: 2670–5.
22 Thoeny RH, Dockerty MB, Hunt AB, Childs DS Jr. A study of ovarian dysgerminoma with emphasis on the role of radiation therapy. *Surg Gynecol Obstet* 1961; **113**: 692–8.
23 Bendall SC, Stewart MH, Menendez P *et al.* IGF and FGF cooperatively establish the regulatory stem cell niche of pluripotent human cells in vitro. *Nature* 2007; **448**: 1015–U3.
24 Li Y. HOXC8-dependent cadherin 11 expression facilitates breast cancer cell migration through trio and rac. *Genes Cancer* 2011; **2**: 880–8.
25 Nakagawa M, Koyanagi M, Tanabe K *et al.* Generation of induced pluripotent stem cells without Myc from mouse and human fibroblasts. *Nat Biotechnol* 2008; **26**: 101–6.
26 Gordan JD, Thompson CB, Simon MC. HIF and c-Myc: sibling rivals for control of cancer cell metabolism and proliferation. *Cancer Cell* 2007; **12**: 108–13.
27 Seki T, Yuasa S, Fukuda K. Derivation of induced pluripotent stem cells from human peripheral circulating T cells. *Curr Protoc Stem Cell Biol* 2011; 11–14. Chapter 4: Unit4A.3.
28 Buganim Y, Faddah DA, Cheng AW *et al.* Single-cell expression analyses during cellular reprogramming reveal an early stochastic and a late hierarchic phase. *Cell* 2012; **150**: 1209–22.

Supporting Information

Additional supporting information may be found in the online version of this article:

Fig. S1. Expression of embryonic stem cell (ESC) markers in abnormally reprogrammed cells (ARCs).

Fig. S2. Impaired differentiation of abnormally reprogrammed cells (ARCs).

Fig. S3. Expression of c-KIT, CD30, and CD45 in common marmoset dysgerminoma-like cells.

Fig. S4. Colony formation of aorta-gonado-mesonephros fibroblasts by the transduction of OCT3/4, SOX2, KLF4, and c-MYC (OSKM) and OSM.

Fig. S5. Validation of genes showing upregulation in abnormally reprogrammed cells (ARCs) compared to normal induced pluripotent stem (iPS) A cells in microarray analysis.

Fig. S6. Integration of reprogramming genes into the genome of common marmoset dysgerminoma-like cells (CM DGs).

Fig. S7. Fluorescence-activated cell sorter analyses to reveal effects of mitomycin C treatment on common marmoset dysgerminoma-like cell lines.

Fig. S8. Fluorescence-activated cell sorter analyses to reveal effects of cisplatin treatment on common marmoset dysgerminoma-like cell lines.

Fig. S9. Fluorescence-activated cell sorter analyses to reveal effects of irradiation on common marmoset dysgerminoma-like cell lines.

Fig. S10. Knockdown of OCT3/4, SOX2, KLF4, or c-MYC by shRNA in common marmoset dysgerminoma-like cell lines.

Fig. S11. Induction of cell death in common marmoset dysgerminoma-like cells by BGJ398.

Table S1. Lentiviral vector integration sites in common marmoset (CM) dysgerminoma-like cells.

Table S2. Human homologs of candidate tumor suppressors located on chromosome 4q in common marmoset (CM).

Video S1. *In vitro* differentiation assay to assess the ability of abnormally reprogrammed cells to differentiate into cardiomyocytes.

Data S1. Materials and Methods.

Inhibition of PTEN Tumor Suppressor Promotes the Generation of Induced Pluripotent Stem Cells

Jiyuan Liao[1], Tomotoshi Marumoto[1,2], Saori Yamaguchi[1], Shinji Okano[3], Naoki Takeda[4], Chika Sakamoto[1], Hirotaka Kawano[1], Takenobu Nii[1], Shohei Miyamato[1], Yoko Nagai[1], Michiyo Okada[1], Hiroyuki Inoue[1,2], Kohichi Kawahara[5], Akira Suzuki[5], Yoshie Miura[1] and Kenzaburo Tani[1,2]

[1]*Division of Molecular and Clinical Genetics, Department of Molecular Genetics, Medical Institute of Bioregulation, Kyushu University, Fukuoka, Japan;* [2]*Department of Advanced Molecular and Cell Therapy, Kyushu University Hospital, Fukuoka, Japan;* [3]*Division of Pathophysiological and Experimental Pathology, Department of Pathology, Graduate School of Medical Sciences, Kyushu University, Fukuoka, Japan;* [4]*Division of Transgenic Technology, Center for Animal Resources and Development, Kumamoto University, Kumamoto, Japan;* [5]*Division of Cancer Genetics, Department of Molecular Genetics, Medical Institute of Bioregulation, Kyushu University, Fukuoka, Japan*

Induced pluripotent stem cells (iPSCs) can be generated from patients with specific diseases by the transduction of reprogramming factors and can be useful as a cell source for cell transplantation therapy for various diseases with impaired organs. However, the low efficiency of iPSC derived from somatic cells (0.01–0.1%) is one of the major problems in the field. The phosphoinositide 3-kinase (PI3K) pathway is thought to be important for self-renewal, proliferation, and maintenance of embryonic stem cells (ESCs), but the contribution of this pathway or its well-known negative regulator, phosphatase, and tensin homolog deleted on chromosome ten (Pten), to somatic cell reprogramming remains largely unknown. Here, we show that activation of the PI3K pathway by the Pten inhibitor, dipotassium bisperoxo(5-hydroxypyridine-2-carboxyl)oxovanadate, improves the efficiency of germline-competent iPSC derivation from mouse somatic cells. This simple method provides a new approach for efficient generation of iPSCs.

Received 28 November 2012; accepted 3 March 2013; advance online publication 9 April 2013. doi:10.1038/mt.2013.60

INTRODUCTION

Mammalian somatic cells can be reprogrammed into induced pluripotent stem cells (iPSCs) by ectopic expression of *Oct3/4* (also known as *Pou5f1*), *Klf4*, and *Sox2* with or without *c-Myc* (hereafter referred to as "OKSM" and "OKS", respectively).[1–4] iPSCs are similar to embryonic stem cells (ESCs) in their morphology, gene expression, and ability to differentiate into the three germ layers *in vitro* and *in vivo*.[1,5] Compared with ESCs, iPSCs avoid ethical controversy and immune rejection and have a great potential to be a cell source for personalized stem cell-based transplantation therapies. However, the efficiency of iPSC generation is quite low (0.01–0.1%), which is one of the obstacles to be overcome.[1–4,6,7] This low efficiency of iPSC generation is considered to be partially due to senescence and apoptosis induced by ectopic expression of OKSM,[8] although the molecular mechanisms involved in somatic cell reprogramming have not been fully elucidated.[1–3,7] Thus, understanding of the molecular mechanisms leading to reprogramming of somatic cells is crucial, and development of a new strategy for efficient iPSC generation is strongly desired.[8]

Numerous studies have shown that the phosphoinositide 3-kinase (PI3K) signaling pathway is required for maintenance of ESC pluripotency by regulating Nanog and Sox2, both of which are transcription factors involved in self-renewal of ESCs.[9–12] In addition, the PI3K pathway is known to be negatively regulated by phosphatase and tensin homolog deleted on chromosome ten (Pten), a well-known tumor suppressor that is deleted or mutated in various types of cancer.[13–16] Recent studies have shown that knockdown of Pten in ESCs promotes self-renewal, as well as cell survival and proliferation,[16–18] indicating that Pten is also involved in the control of stem cell behavior through PI3K regulation.

Here, we report that transient inhibition of Pten by its inhibitor during the process of reprogramming mouse embryonic fibroblasts (MEFs) promotes their proliferation and enhances the efficiency of germline-competent iPSC generation by ectopic expression of OKSM.

RESULTS

To examine whether inhibition of Pten facilitates the reprogramming process for iPSC generation, we first retrovirally transduced OKSM into MEFs lacking Pten (Pten$^{-/-}$ MEFs)[19] and cultured these cells on mitomycin C (MMC)-treated SNL feeders (a SIM mouse embryo-derived thioguanine and ouabain resistant (STO) cell line transformed with neomycin resistance and mouse leukemia inhibitory factor genes) in mouse ESC medium. At about 7 days after OKSM transduction into Pten$^{-/-}$ MEFs, ESC-like round-shaped colonies were observed (**Figure 1a**). We examined the expression of stage-specific mouse embryonic antigen1 (SSEA1), a marker of mouse ESCs, by immunocytochemistry (**Figure 1b,c**).[20] The number of SSEA1^{+} colonies induced by OKSM significantly increased in Pten$^{-/-}$ MEF cultures (103 ± 2) compared with that in Pten$^{+/-}$ and wild-type MEF cultures (40 ± 9 and 21 ± 9, respectively; **Figure 1c**,

The first two authors contributed equally to this work.

Correspondence: *Kenzaburo Tani, Division of Molecular and Clinical Genetics, Department of Molecular Genetics, Medical Institute of Bioregulation, Kyushu University, 3-1-1 Maidashi, Higashi-ku, Fukuoka, 812–8582, Japan. E-mail: taniken@bioreg.kyushu-u.ac.jp*

left panel). Similar results were obtained when OKS were transduced (15±4 for Pten$^{-/-}$ MEFs, 6±2 for Pten$^{+/-}$ MEFs and 2±1 for wild-type MEFs; **Figure 1c**, right panel).

To confirm that SSEA1$^+$ colonies were derived from a single cell, and not from cell clusters, we replated fewer OKSM-transduced Pten$^{-/-}$ MEFs onto MMC-treated SNL feeders (100 cells per well in a six-well plate) in ESC medium. At 14 days after retroviral transduction, the number of alkaline phosphatase-positive (AP$^+$) colonies was counted. As a result, 71±12 AP$^+$ colonies were generated from Pten$^{-/-}$ MEFs, whereas only 8±1 colonies were generated from wild-type MEFs (**Figure 1d**, left panel), indicating that ~70% of OKSM-transduced Pten$^{-/-}$ MEFs had the potential to become iPSCs. Similar results were obtained when OKS were transduced into Pten$^{-/-}$ MEFs (**Figure 1d**, right panel). These results strongly indicated that the deficiency of Pten significantly increased the number of iPSCs generated by transduction of OKSM or OKS.

Loss of Pten has been shown to activate the PI3K-Akt pathway.[13,21] We next activated the PI3K pathway by expression of phosphatase-deficient Pten mutants that contained a Cys-124 to serine substitution at the phosphatase catalytic center (CS-Pten),[22] or the active myristoylated form of Akt (myr-Akt),[23] and then the efficiency of iPSC generation from wild-type MEFs by OKSM transduction was examined. We observed significantly more AP$^+$ colonies generated from MEFs expressing CS-Pten+OKSM or myr-Akt+OKSM compared with those generated from the control (354±41, 355±10 and 231±25, respectively) (**Figure 2a**). These results indicated that activation of the PI3K pathway in MEFs enhanced the generation of iPSCs by co-expression of OKSM.

It is thought that continuous activation of the PI3K pathway may cause transformation of cells.[24] Therefore, to efficiently and safely generate iPSCs, transient activation of the PI3K pathway combined with transduction of OKSM might be desirable. To establish transient activation of the PI3K pathway, we used a Pten inhibitor, dipotassium bisperoxo(5-hydroxypyridine-2-carboxyl)oxovanadate [bpV(HOpic)],[25] during the process of iPSC generation (from day 0 to 10 after transduction) (**Figure 2b**). The bpV(HOpic) concentration was considered optimal at 100 nmol/l, which was determined by analyzing the activation status of Akt in MEFs by western blotting (**Supplementary Figure S1** and **Supplementary Materials and Methods**). MEFs cultured in medium containing 100 nmol/l bpV(HOpic) were transduced with OKSM, resulting in generation of ESC-like colonies (bpV-iPSCs) on day 14 after transduction (**Figure 2b,e**, left panel). After isolation of these ESC-like colonies on day 14 after transduction, eight bpV-iPSC lines were established and expanded in conventional ESC medium on SNL feeders and then characterized further (**Supplementary Table S1**). Reverse transcription PCR showed that all of the bpV-iPSC lines examined (8/8) expressed ESC markers such as endogenous *Oct3/4*, *Sox2*, and *Nanog* (**Figure 2d**). In addition, bpV-iPSC lines were positive for AP activity and SSEA1 staining (**Figure 2e**, middle and right panels, respectively). It should be noted that the efficiency of iPSC generation from OKSM-transduced MEFs in the presence of bpV(HOpic) was much higher than that from the untreated control (353±42 versus 189±32; **Figure 2c**, left panel). Furthermore, inhibition of the PI3K pathway by LY294002,[26] a reversible inhibitor of all classes of PI3Ks, resulted in a sharp decrease of the efficiency of iPSC generation (20±11; **Figure 2c**, left panel). Similar results were obtained when OKS were

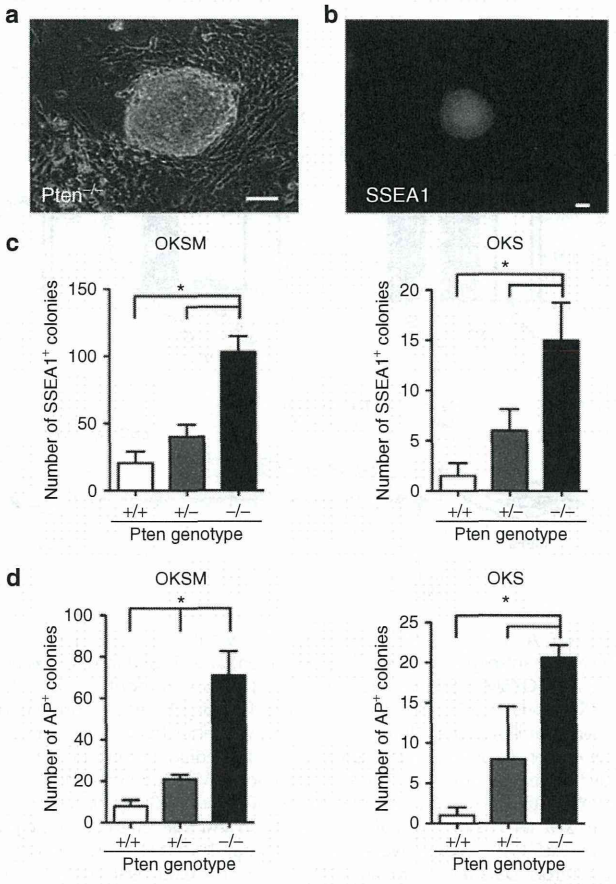

Figure 1 Loss of Pten promotes reprogramming of MEFs into iPSCs. (**a**) Representative image of an iPSC colony derived from Pten$^{-/-}$ MEFs by transduction of mouse OKSM. Scale bar = 100 µm. (**b**) Immunocytochemical staining of SSEA1 on iPSCs induced by transduction of OKSM into Pten$^{-/-}$ MEFs. Scale bar = 0.2 mm. (**c**) Counts of SSEA1$^+$ colonies. A total of 5,000 (OKSM) or 50,000 (OKS) retrovirally transduced MEFs with Pten$^{+/+}$, Pten$^{+/-}$, or Pten$^{-/-}$ genotypes were transferred onto feeders on day 4 after transduction. SSEA1$^+$ colonies were counted on day 14 (OKSM, left) and day 28 (OKS, right) after transduction. Data are the mean ± SD (n = 3), *P < 0.05 versus wild type. (**d**) Counts of AP$^+$ colonies derived from single cells. A total of 100 MEFs (OKSM or OKS) with Pten$^{+/+}$, Pten$^{+/-}$, or Pten$^{-/-}$ genotypes were transferred onto feeders on day 4 after transduction. AP$^+$ colonies generated from Pten$^{+/+}$, Pten$^{+/-}$, or Pten$^{-/-}$ MEFs transduced with OKSM (left) or OKS (right) were counted on day 12 (OKSM) and day 28 (OKS) after transduction. Data are the mean ± SD (n = 3 or more), *P < 0.05 versus wild type. iPSC, induced pluripotent stem cell; MEF, mouse embryonic fibroblast.

transduced in the presence of bpV(HOpic) (89±11 versus 60±5; **Figure 2c**, right panel). Moreover, the emergence of SSEA1$^+$ colonies from MEFs transduced with OKSM was enhanced by bpV(HOpic) treatment (n = 3, P < 0.05; **Supplementary Figure S2**).

These results were further confirmed by experiments using MEFs carrying the green fluorescent protein (GFP) gene under the control of the *Nanog* promoter (*Nanog*-GFP MEFs).[12] We found that transient treatment with bpV(HOpic) significantly increased the number of *Nanog*-GFP$^+$ colonies from MEFs transduced with OKSM or OKS under a feeder-free condition (n > 3, P < 0.05; **Figure 3a**). These results strongly indicated that inhibition of Pten promoted the efficiency of iPSC generation by transduction of OKSM or OKS.

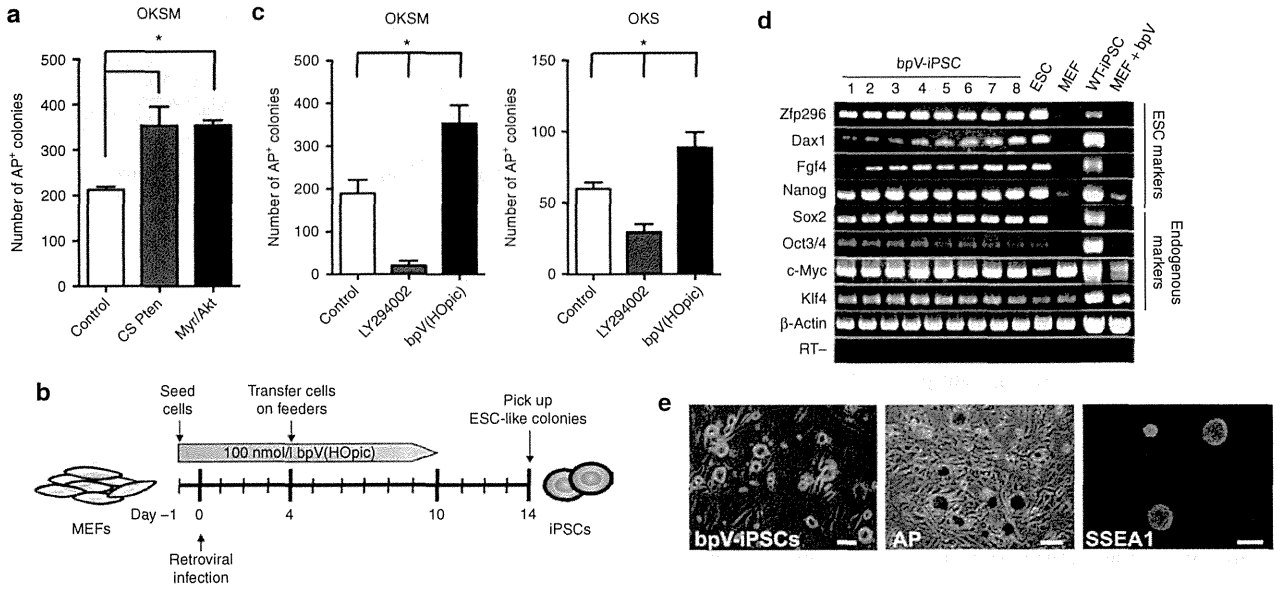

Figure 2 Activation of the PI3K-Akt pathway enhances iPSC generation. (**a**) Counts of AP+ colonies formed by transduction of OKSM combined with the dominant-negative form of Pten (CS-Pten) or activated form of Akt (myr-Akt) into MEFs. Wild-type MEFs (1×10^5) were transduced with OKSM (control, left), OKSM+CS-Pten (middle), or OKSM+myr-Akt (right). Cells (5,000) were transferred onto SNL feeders on day 4 after transduction and cultured in ESC medium. AP+ colonies were counted on day 14 after transduction. Data are the mean ± SD ($n = 3$), $^*P < 0.05$ versus control. (**b**) Experimental scheme for iPSC generation. MEFs (1×10^5) were infected with retroviruses carrying OKSM on day 0. Cells (5,000) were transferred onto SNL feeders on day 4 after transduction and cultured in ESC medium containing 100 nmol/l bpV(HOpic). Colonies were collected based on ESC-like morphology on day 14 after transduction. The Pten inhibitor bpV(HOpic) was added from day –1 to 10. (**c**) Counts of AP+ colonies formed by transduction of OKSM or OKS into MEFs in the presence of LY294002 or bpV(HOpic). A total of 5,000 (OKSM) or 50,000 (OKS) retrovirally transduced MEFs were transferred onto SNL feeders on day 4 after transduction and then cultured in the presence of 100 nmol/l bpV(HOpic) or 5 μmol/l LY294002 for 10 (OKSM) or 28 days (OKS). AP+ colonies were counted on day 10 (OKSM, left panel) and day 28 (OKS, right panel). AP+ colonies generated without drugs were used as controls. Data are the mean ± SD ($n = 3$), $^*P < 0.05$ versus controls. (**d**) Characteristics of bpV-iPSCs *in vitro*. The expression of ESC marker genes in bpV-iPSCs (OKSM) was examined by RT PCR (bpV-iPSC clones 1–8). Mouse β-actin was used as a loading control. The RT (–) control is shown at the bottom. (**e**) Representative images of bpV-iPSC colonies (left panel), AP staining (middle panel), and SSEA1 staining (right panel). Scale bars = 100 μm. ESC, embryonic stem cell; iPSC, induced pluripotent stem cell; MEF, mouse embryonic fibroblast; RT, reverse transcription.

It has been reported that the use of PS48, a small molecule activator of 3′-phosphoinositide–dependent kinase-1 (PDK1) that is involved in the PI3K pathway, can enhance the reprogramming efficiency for iPSC generation from human cells.[27] We therefore examined whether bpV(HOpic) or PS48 could further enhance the reprogramming efficiency. We found that a significantly higher number of AP+ colonies were formed from bpV(HOpic)-treated MEFs compared with that from PS48-treated MEFs ($n = 3$, $P < 0.05$; **Supplementary Figure S3**), indicating that inhibition of Pten by bpV(HOpic) might be a better approach than activation of PDK1 by PS48 for the enhancement of reprogramming.

To exclude the possibility that nonspecific effects of bpV(HOpic) had affected the iPSC generation, we also tested other specific Pten inhibitors such as SF1670 and bpV(Phen). As a result, the number of AP+ colonies appeared to significantly increase on day 10 after transduction in the presence of SF1670 or bpV(Phen) (**Supplementary Figure S4**).

It has been reported that various kinds of chemicals and supplements, such as histone deacetylase inhibitors, valproic acid (VPA), MAPK/ERK kinase inhibitors + glycogen synthase kinase 3β (GSK3β) inhibitors (2i), and vitamin C (Vc), enhance the reprogramming efficiency of somatic cells into iPSCs.[6,28–30] Therefore, various combinations of bpV(HOpic) were tested with these compounds, such as bpV(HOpic)+Vc, bpV(HOpic)+2i, and bpV(HOpic)+VPA. We found that combined use of bpV(HOpic) with each compound significantly increased the number of AP+ or *Nanog*-GFP+ colonies generated from OKSM-transduced MEFs ($n = 3$, $P < 0.05$; **Supplementary Figure S5** and **Supplementary Materials and Methods**). In particular, bpV(HOpic)+VPA strongly enhanced the reprogramming efficiency by more than fourfold compared with that of bpV(HOpic) alone (12±4 versus 48±7; **Supplementary Figure S5**).

Next, we examined the characteristics of bpV-iPSCs. Bisulfite genomic sequencing analyses were performed to examine epigenetic modification of pluripotency-associated promoter regions such as *Nanog* and *Oct3/4* genes.[1,2,12,31] The promoters of *Nanog* and *Oct3/4* genes in OKSM- and OKS-transduced bpV-iPSCs were less methylated than those in MEFs, which was similar to those in ESCs (**Figure 3b** and **Supplementary Figure S6**), suggesting that similar DNA methylation patterns of pluripotency genes, such as Nanog and Oct3/4, stably maintained the undifferentiated state of bpV-iPSCs.

In addition, karyotype analyses showed that the chromosomal status of bpV-iPSCs was normal over 15 passages (**Supplementary Figure S7**), indicating that transient activation of the PI3K pathway by a Pten inhibitor, bpV(HOpic), did not affect chromosomal stability in the process of reprogramming.

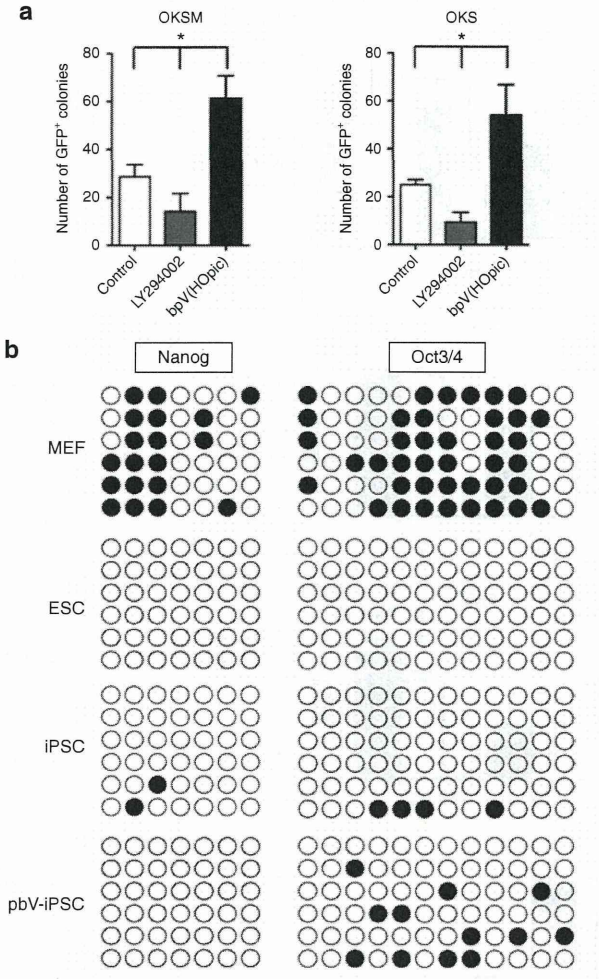

Figure 3 Addition of bpV(HOpic) improves the reprogramming of *Nanog*-GFP MEFs by OKSM or OKS. (**a**) Counts of *Nanog*-GFP$^+$ colonies formed by transduction of OKSM or OKS into MEFs in the presence of LY294002 or bpV(HOpic). *Nanog*-GFP MEFs were retrovirally transduced with OKSM (left panel) or OKS (right panel) and then cultured in the presence of 5 µmol/l LY294002 or 100 nmol/l bpV(HOpic) for 9 days (from day 5 to 14 after transduction, left panel) or 33 days (from day 5 to 38 after transduction, right panel). The number of GFP$^+$ colonies was counted by observation under an immunofluorescence microscope. Data are the mean ± SD ($n = 12$ for LY294002- or bpV(HOpic)-treated groups and $n = 6$ for the control group), $^*P < 0.05$. (**b**) DNA methylation analysis of the promoter regions for endogenous *Nanog* and *Oct3/4* genes. Genomic DNA from wild-type MEFs, mouse ESCs, wild-type iPSCs, and bpV-iPSCs (OKSM) were analyzed by bisulfite sequencing. Open and closed circles indicate unmethylated and methylated CpG islands, respectively. ESC, embryonic stem cell; iPSC, induced pluripotent stem cell; MEF, mouse embryonic fibroblast.

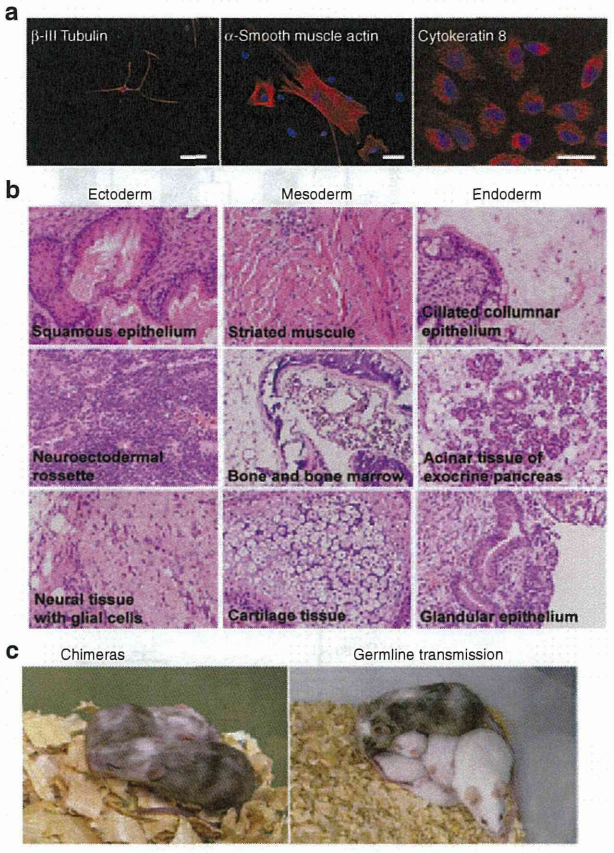

Figure 4 Pluripotency of bpV-iPSCs. (**a**) *In vitro* differentiation ability of bpV-iPSCs. After EB formation for 7 days, EBs were transferred onto 0.1% gelatin-coated dishes, cultured for another 6 days, fixed, and then processed for immunocytochemistry using antibodies against β-III tubulin (ectoderm marker, left panel), α-smooth muscle actin (mesoderm marker, middle panel), and cytokeratin 8 (endoderm marker, right panel). Scale bars = 50 µm. (**b**) *In vivo* differentiation ability of bpV-iPSCs. Hematoxylin-eosin staining of tissue sections showing teratomas composed of mature tissues derived from the three embryonic germ layers. Magnification ×200. (**c**) Contribution of bpV-iPSCs to chimeric mice. Injection of bpV-iPSCs derived from ICR mice into C57BL/6 blastocysts led to the generation of chimeric mice (left panel). Offspring (chimera male × ICR female) were white, indicating germline transmission of bpV-iPSCs (right panel). iPSC, induced pluripotent stem cell.

We next examined *in vitro* and *in vivo* differentiation potentials of bpV-iPSCs. bpV-iPSC differentiation was induced by embryoid body (EB) formation *in vitro*. Immunocytochemical analysis revealed that EB-formed cells expressed lineage markers of the ectoderm (β-III tubulin), mesoderm (α-smooth muscle actin), and endoderm (cytokeratin 8) (**Figure 4a**). We then performed a teratoma formation assay *in vivo*. One-million bpV-iPSCs were injected into the testes and backs of SCID mice. At 4–5 weeks after injection, we observed tumor formation. Histological analyses by hematoxylin-eosin staining showed that the tumors contained various derivatives of the three germ layers, indicating development of a well-differentiated teratoma (**Figure 4b**). Moreover, bpV-iPSCs contributed to somatic tissue formation in chimeric mice and showed a germline transmission capability (**Figure 4c**). These results strongly indicated that bpV-iPSCs possessed pluripotency *in vitro* and *in vivo*.

Next, we attempted to elucidate the mechanisms that promoted iPSC generation by the Pten inhibitor. We first examined the effect of bpV(HOpic) on the reprogramming time window by transduction of OKSM or OKS into *Nanog*-GFP MEFs. We found that the reprogramming time window was not affected by the addition of bpV(HOpic), although the number of GFP$^+$ cells was increased on around day 10 (OKSM) and day 15 (OKS) after transduction (**Figure 5a**).

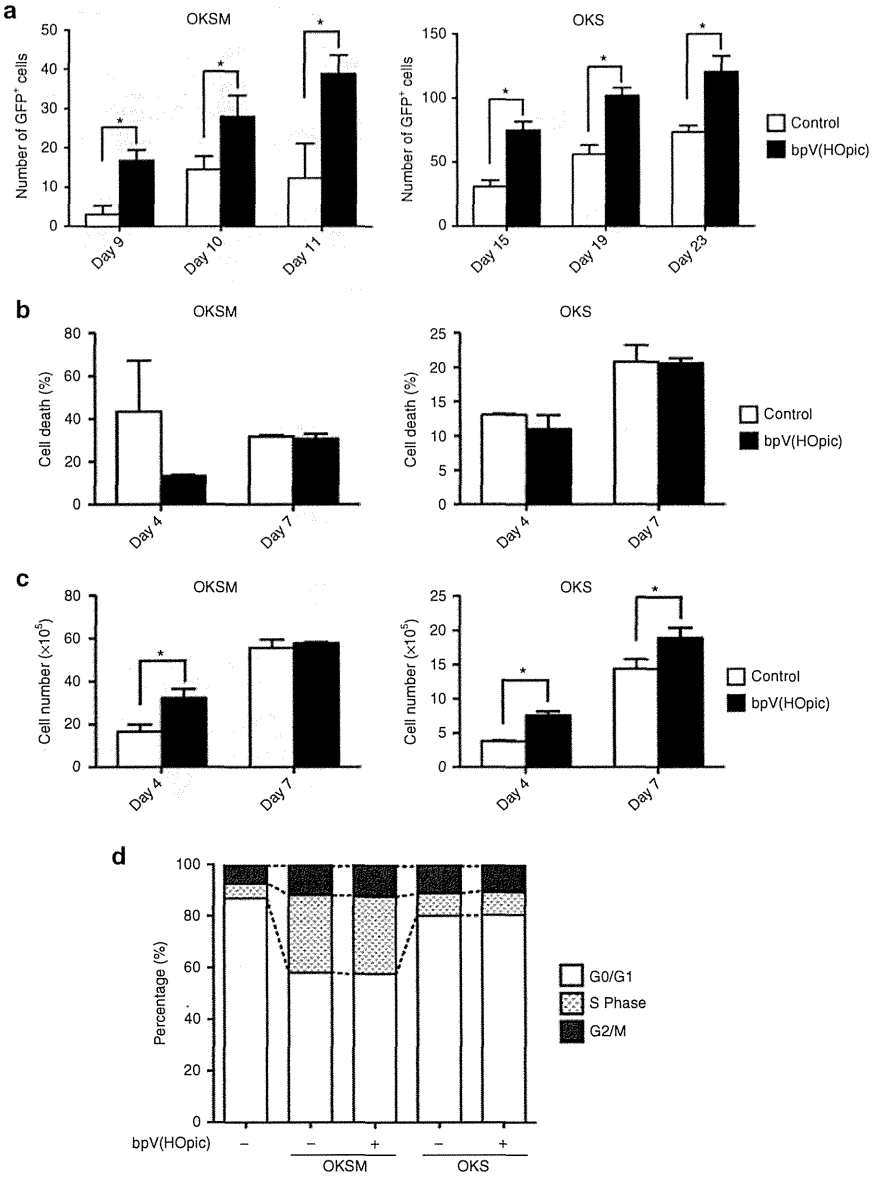

Figure 5 Effects of bpV(HOpic) on survival, proliferation, and reprogramming of MEFs. (**a**) Promotion of reprogramming by bpV(HOpic). *Nanog*-GFP MEFs were retrovirally transduced with OKSM (upper panel) or OKS (lower panel) and then cultured in the presence (black bar) or absence (white bar) of bpV(HOpic). The number of GFP$^+$ cells was counted by observation under an immunofluorescence microscope at the indicated time points after transduction. Data are the mean ± SD (n = 3), *P < 0.05. (**b**) Analysis of cell death. OKSM- (left panel) or OKS- (right panel) transduced MEFs were cultured with or without 100 nmol/l bpV(HOpic) for 4 or 7 days. The annexin V$^+$ cell population was analyzed by flow cytometry. Data are the mean ± SD (n = 3). (**c**) Effects of bpV(HOpic) on cell proliferation. The number of OKSM- (left panel) or OKS- (right panel) transduced MEFs cultured with or without 100 nmol/l bpV(HOpic) for 4 or 7 days was counted. Data are the mean ± SD (n = 3), *P < 0.05. (**d**) Cell cycle analysis. OKSM- or OKS-transduced MEFs were cultured in the presence of 100 nmol/l bpV(HOpic) for 4 days, and then a BrdU assay was performed. MEFs and OKSM- or OKS-transduced MEFs without bpV(HOpic) treatment were used as controls. Data are the mean ± SD (n = 3). GFP, green fluorescent protein; MEF, mouse embryonic fibroblast.

To further address how the efficiency of iPSC generation was enhanced by Pten inhibition, we examined cell death, cell cycle distribution, and proliferation affected by bpV(HOpic). Cell survival of OKSM- and OKS-transduced MEFs treated with bpV(HOpic) in the process of reprogramming was assessed using annexin V staining. We did not observe any significant increase or decrease in cell death induced by bpV(HOpic) at the indicated time points (**Figure 5b**), although cell death on day 4 after transduction tended to be inhibited in the presence of bpV(HOpic). However, we found that the proliferation rate of OKSM- and OKS-transduced MEFs treated with bpV(HOpic) was slightly higher than that of the untreated control (**Figure 5c**), although the data from OKSM-transduced MEFs on day 7 after transduction showed no effect on proliferation induced by bpV(HOpic). These

data indicated that bpV(HOpic) treatment slightly promoted cell proliferation, particularly during the early phase of reprogramming of OKSM- and OKS-transduced MEFs. However, the cell cycle distribution was not changed significantly (**Figure 5d**). These results indicated that the enhancement of iPSC generation by Pten inhibition was associated with slightly accelerated cell proliferation during the early phase of reprogramming.

DISCUSSION

It is known that the efficiency of iPSC generation by retroviral transfer of reprogramming factors into MEFs is ~0.1–1%.[1–4,6,7] In this study, we have developed a novel method that enhances the reprogramming efficiency of OKSM-transduced mouse somatic cells by transient activation of the PI3K pathway using a Pten inhibitor, bpV(HOpic). The efficiency of AP^+ cell generation from OKSM-transduced MEFs by the addition of bpV(HOpic) was ~7% (**Figure 2c**, left panel). This high proportion of AP^+ cells was surprising, but there was a possibility that insufficiently reprogrammed cells were included in the AP^+ population. Therefore, we also examined the efficiency of $SSEA1^+$ cell generation from MEFs. The proportion of $SSEA1^+$ cells generated from OKSM-transduced MEFs treated with bpV(HOpic) was ~3% ($n = 3$, $P < 0.05$; **Supplementary Figure S2**), strongly suggesting the ability of bpV(HOpic) to enhance iPSC generation. It should also be noted that combined use of bpV(HOpic) with VPA further improved iPSC generation (**Supplementary Figure S5b**).

The mechanisms of bpV(HOpic) treatment, which increase the efficiency of iPSC generation, are considered to be crucial. We have shown that treatment with LY294002 from day 0 to 10 after OKSM transduction inhibited the efficiency of iPSC generation (**Figure 2c**), whereas expression of the activated form of Akt (myr-Akt)-enhanced iPSC generation (**Figure 2a**). Thus, it is conceivable that activation of the PI3K-Akt pathway due to inhibition of Pten by bpV(HOpic) at least in part plays a role in the reprogramming process.

Several molecules downstream of the PI3K-Akt pathway are responsible for critical biological phenomena such as self-renewal, and cell survival and proliferation. It has been reported that *c-Myc* and its downstream target, cyclin D, are activated by the PI3K-Akt pathway,[32] which leads to acceleration of the cell cycle. Another report has described that Akt inhibits cell cycle inhibitory molecules, p21 and p27.[8,33] This evidence indicates that activation of the PI3K-Akt pathway promotes cell proliferation. Indeed, MEFs treated with bpV(HOpic) showed a slightly higher rate of proliferation (**Figure 5b**). Previous reports have described that promotion of cell proliferation results in the enhancement of iPSC generation.[34] Thus, the acceleration of cell proliferation caused by the treatment with bpV(HOpic) may be associated with the activation of cell cycle molecules, which leads to the elevation of the efficiency of iPSC generation from somatic cells.

Several reports have shown that GSK3β is a key regulator of cellular fate and a participant in differentiation events during embryonic development through the Wnt/GSK3β/β-catenin signaling pathway.[35] Phosphorylation of GSK3β by Akt allows translocation of β-catenin into the nucleus, which activates transcription factors such as *c-Myc* and *Nanog* and promotes reprogramming.[29,36] Therefore, the use of bpV(HOpic) might inhibit GSK3β through activation of the PI3K-Akt pathway, resulting in the enhancement of iPSC generation.

Recently, treatment with 0.3 μmol/l LY294002, a PI3K pathway inhibitor, from day 1 to 3 after OKSM transduction was shown to enhance the efficiency of iPSC generation from MEFs.[37] However, in our study, treatment with 5 μmol/l LY294002 from day 0 to 10 after OKSM transduction inhibited the efficiency of iPSC generation (**Figure 2c**). The discrepancy between these data might be due to the difference in drug concentrations and/or the duration of drug treatment used for iPSC generation.

It has been reported that the efficiency of reprogramming is enhanced by increased cell proliferation and survival by inhibition of the p53-p21 pathway and *Ink4a/Arf* locus.[8,33,34,38–42] Indeed, use of the p53 inhibitor pifithrin-α hydrobromide (PFTα) tended to show a higher reprogramming efficiency (**Supplementary Figure S8**). However, p53 was slightly accumulated in OKSM-transduced MEFs treated with bpV(HOpic) (**Supplementary Figure S9**), indicating that promotion of iPSC generation by bpV(HOpic) was not due to reduced p53 protein levels. Further investigation is needed to reveal the significance of slight p53 stabilization in OKSM-transduced MEFs treated with bpV(HOpic).

Interestingly, for cell proliferation, previous reports have shown that mitochondrial oxidation is generally used in differentiated somatic cells, whereas glycolysis is mainly used in pluripotent cells.[27,43] In addition, it has been shown that modulation of cell metabolism from mitochondrial oxidation to glycolysis plays an important role in the process of iPSC generation.[27,43,44] Because PI3K signaling is known to be a potent regulator of cellular metabolism,[45] the possibility that inhibition of Pten by bpV(HOpic) induces a change of metabolic pathways from mitochondrial oxidation to glycolysis should also be carefully examined in the future.

Because continuous activation of the PI3K pathway causes transformation of cells,[46] bpV(HOpic) treatment may cause the emergence of cancer cells. However, iPSCs generated in the presence of bpV(HOpic) could be readily and stably expanded over a long term under conventional ESC culture conditions (>15 passages) and exhibited a normal karyotype (**Supplementary Figure S7**). Furthermore, they could directly differentiate into the three germ layers *in vitro* and formed teratomas *in vivo*. In mice, injection of these bpV-iPSCs into C57BL/6 host blastocysts resulted in the generation of healthy chimeric mice showing a germline transmission capability (**Figure 4**). Out of 11 chimeric mice aged over 1 year, nine mice did not survive owing to unknown reasons, and only one mouse formed a teratoma in the left leg (data not shown). Teratoma formation in a bpV-iPSC chimeric mouse might be influenced by reactivation of reprogramming factors or transient activation of the PI3K pathway in the process of reprogramming. In addition, some of the bpV-iPSCs injected into blastocysts might remain in an undifferentiated state. These possibilities need to be carefully considered when iPSC-based cell replacement therapies are conducted for regenerative medicine in the future.

MATERIALS AND METHODS

Plasmids. pMXs-based retroviral vectors for mouse *Oct3/4*, *Klf4*, *Sox2*, and *c-Myc* were obtained from Addgene (Cambridge, MA).[47] pMXs vectors encoding a mutant derivative of Pten containing a Cys-124 to serine

substitution (*CS-Pten*),[22] *myr-Akt*, or *GFP* genes were gifts from Akira Suzuki (Kyushu University, Fukuoka, Japan).

Cell culture. PLAT-E cells for production of retroviruses were kindly provided by Dr. Toshio Kitamura (Tokyo University, Tokyo, Japan) and maintained in Dulbecco's modified Eagle's medium (DMEM; Invitrogen, Carlsbad, CA) containing 10% fetal bovine serum (FBS; Invitrogen), 1 mg/ml puromycin (InvivoGen, San Diego, CA), and 10 μg/ml blasticidin S (InvivoGen).[48] MEFs were isolated from pregnant mice at gestational day 12 (Crlj: CD1, Charles River, Japan; *Nanog*-GFP Mouse, Rikken, Japan) and expanded in fibroblast medium consisting of DMEM/10% FBS with 1% antibiotic-antimycotic mixed stock solution (Nacalai Tesque, Kyoto, Japan). Pten-deficient MEFs were kindly provided from Dr. Akira Suzuki (Kyushu University, Fukuoka, Japan).[19] SNL feeders and MEFs were cultured in DMEM/10% FBS with antibiotics on 0.1% gelatin-coated dishes at 37 °C with 5% CO_2. SNL feeders were treated with 12 μg/ml MMC (Kyowa Hakko Kirin, Tokyo, Japan) for around 2 hours before coculture with iPSCs. Mouse iPSCs were cultured on gelatin-coated plates with MMC-treated SNLs in mouse ESC medium consisting of knockout DMEM containing 1000 U/ml leukemia inhibitory factor (Wako, Osaka, Japan), 2 mmol/l L-glutamine (Nacalai Tesque), 10% FBS, 0.1 mmol/l 2-mercaptoethanol (Sigma-Aldrich, St Louis, MO), 1% nonessential amino acids (Invitrogen), and 50 IU/ml penicillin and 50 mg/ml streptomycin mixed solution (Nacalai Tesque).

Retrovirus production and iPSC generation. For retroviral production, PLAT-E cells were seeded at 3.3×10^6 cells per 100 mm dish. The following day, 9 μg pMXs-based retroviral vectors for expression of GFP, *Oct3/4*, *Klf4*, *Sox2*, or *c-Myc* were individually introduced into PLAT-E cells using FuGENE 6 transfection reagent (Roche Diagnostics, Indianapolis, IN). After 24 hours, the medium was replaced with 10 ml DMEM/10% FBS, and the supernatant was collected on the following day. On day 0, equal volumes of supernatants from PLAT-E cell cultures containing retroviruses carrying each factor were mixed, and then 1×10^5 (OKSM) – 1×10^6 (OKS) ICR-MEFs or 8×10^4 (OKSM) – 1×10^6 (OKS) Nanog-GFP MEFs were incubated with the mixture. At 4 days after infection, the cells were transferred onto MMC-treated SNL feeders and cultured in ESC medium. Using 35-mm dishes, 5,000 OKSM-transduced and 50,000 OKS-transduced cells were transferred onto SNL feeders. AP^+ and $SSEA1^+$ colonies were examined on day 14 for OKSM-transduced cells, and on day 28 for OKS-transduced cells. To examine the efficiency of iPSC generation from single cell population, 100 of OKSM-transduced cells or 100 of OKS-transduced cells were transferred onto MMC-treated SNL feeders on day 4 after transduction, and their AP activity was examined on days 14 (OKSM) and 28 (OKS), respectively.

Regulation of the PI3K-Akt pathway. To activate the PI3K-Akt pathway, MEFs were retrovirally transduced with a dominant-negative mutant type of Pten (CS-Pten)[22] or activated form of myristoylated Akt (myr-Akt).[23] Moreover, to activate the PI3K-Akt pathway with the Pten inhibitor, MEFs were treated with bpV(HOpic) (100 nmol/l; Calbiochem, Darmstadt, Germany), bpV(Phen) (100 nmol/l; Calbiochem), SF1670 (500 nmol/l; Cellagen Technology, San Diego, CA), or PS48 (5 μmol/l; Wako). Then, to inhibit the PI3K-Akt pathway, cells were treated with LY294002 (5 μmol/l; Santa Cruz Biotechnology, Heidelberg, Germany).

AP staining. AP staining was performed using an Alkaline Phosphatase Kit (Sigma-Aldrich). Colonies grown in 35-mm dishes were fixed in a fixative solution for 30 seconds at room temperature and then washed twice with deionized water for 45 seconds. Fixed cells were incubated with the AP staining solution while protected from light for 1 hour at room temperature and then washed twice with deionized water for 2 minutes. The samples were then observed by optical microscopy (Axiovert 135; ZEISS, Deutschland, Germany).

Immunocytochemical staining. Cells were fixed with 4% paraformaldehyde in phosphate-buffered saline (PBS) for 30 minutes and then washed extensively with PBS. The cells were then permeabilized with 0.3% Triton X-100 in PBS for 5 minutes, followed by blocking with 3% bovine albumin serum in PBS. Staining was carried out by incubation with an anti-SSEA1 antibody (Santa Cruz Biotechnology) overnight at 4 °C. After extensive washing, an antimouse Alexa546 antibody (Invitrogen) was applied for 1 hour at room temperature, and then the cells were counterstained with 4,6-diamindino-2-phenylindole-2 (Invitrogen). Images were obtained by immunofluorescence microscopy (BZ-9000, KEYENCE, Osaka, Japan).

Reverse transcription PCR. Total RNA was extracted from cultured cells using an RNeasy kit (Qiagen, Courtaboeuf, France), and cDNA was synthesized using a reverse transcription system (Invitrogen). PCR was performed using KOD FX DNA polymerase (Toyobo, Tokyo, Japan) according to the manufacturer's instructions. Primer sequences are described in **Supplementary Tables S2** and **S3**. PCR products were size fractionated on 1% agarose gels. β-actin was used as a loading control.

Bisulfite sequencing and karyotype analysis. Genomic DNA from mouse ESCs, MEFs, and bpV-iPSCs was extracted with a DNeasy Blood & Tissue Kit (Qiagen) and then treated with sodium bisulfite using a BisulFast DNA Modification Kit (Toyobo). Treated DNA was purified using an EZ kit (Zymo Research, Orange, CA). Then, *Nanog* and *Oct3/4* gene promoter regions[49] were amplified by PCR using primers shown in **Supplementary Table S4**. PCR products were inserted into a pGEM-T easy vector (Promega, Madison, WI) and then sequenced using M13 primers. Karyotype analysis was performed at the ICLAS Monitoring Center, Central Institute for Experimental Animals.

Spontaneous differentiation* in vitro *and immunocytochemistry. The pluripotency of bpV-iPSCs was assessed by an *in vitro* differentiation assay. Briefly, single cells were harvested by trypsinization, and 1×10^6 cells were cultured on low adhesion plates in mouse ESC medium without leukemia inhibitory factor. Half medium volumes were exchanged every day, and EBs were allowed to grow for 6–7 days in suspension. Then, EBs were trypsinized and replated onto 0.1% gelatin-coated dishes and cultured for another 7 days (ectoderm) or 14 days (endoderm and mesoderm). Spontaneous differentiation was examined by immunocytochemistry using antibodies against cytokeratin 8 (Invitrogen), α-smooth muscle actin (Sigma, St Louis, MO), and β-III tubulin (Sigma). The samples were observed by immunofluorescence microscopy (BZ-9000).

Teratoma formation assay. The bpV-iPSCs (1×10^6) were resuspended in 50 μl PBS and then injected into the testis or back of SCID mice (Charles River Laboratories). At 4–8 weeks after injection, formed tumors were removed and fixed in 4% paraformaldehyde/PBS overnight at 4 °C. Tumor tissues were embedded in paraffin. Tissue blocks were sectioned at 3 μm and stained with hematoxylin-eosin. All animal experiments were approved by the Animal Committees at Kyushu University and Kumamoto University, Japan.

Generation of chimeric mice. To generate chimeric mice derived from bpV-iPSCs, C57BL/6 host blastocysts injected with bpV-iPSCs were transplanted into the uteri of surrogate ICR mice. Detailed protocols have been described before.[50]

Proliferation and cell death analyses. OKSM- or OKS-transduced MEFs (1×10^5) were cultured in DMEM/10% FBS with or without bpV(HOpic). On days 4 and 7, cells were harvested and counted with a TC10 automated cell counter (Bio-Rad, Hercules, CA) to determine the cell number. The cells were then stained with annexin V-APC (BD Pharmingen, San Diego, CA), and the population of annexin V^+ dead cells was analyzed by flow cytometry (FACS Verse; BD Biosciences, San Jose, CA).

BrdU assay. The BrdU incorporation assay was performed with BrdU FLOW Kits according to the manufacturer's instructions (BD Pharmingen). Briefly, OKSM- or OKS-transduced MEFs were cultured in the presence